

Abstract

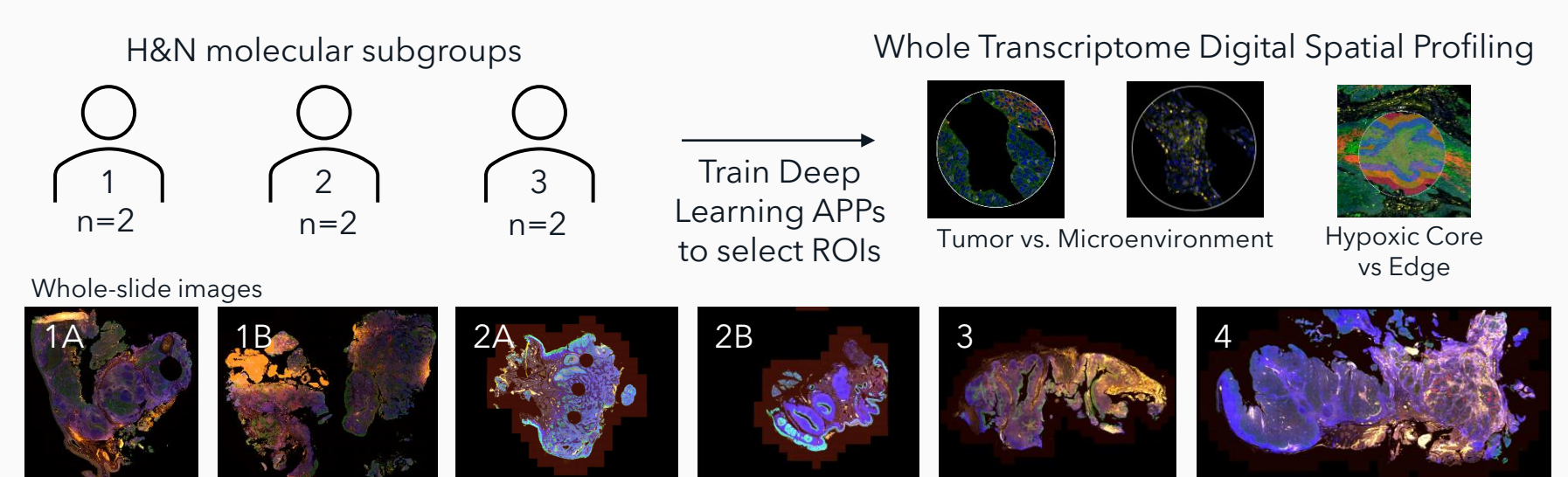
Background: Head and neck cancer (HNC) is a heterogeneous group of malignancies that arise from the mucosal surfaces of the upper aerodigestive tract. The tumor microenvironment (TME) of HNC is characterized by the presence of immune cells, stromal cells, and extracellular matrix components. A key feature of the TME is hypoxia, which promotes tumor growth, invasion, and metastasis by altering the expression of genes involved in angiogenesis, cell survival, and metabolism. Understanding the complex interplay between hypoxia and immune infiltrates in the TME of HNC is crucial for the development of novel therapeutic strategies for the treatment of this disease. Whole transcriptome analysis by digital spatial profiling is an excellent method of probing the TME, but assessing large cohorts can be time consuming. Automating a profiling workflow to reduce hands-on time and region of interest (ROI) selection bias will enable exploration of large cohorts to identify mechanisms of action, potential drug targets, and biomarkers.

Methods: We developed an optimized spatial multi-omic workflow to enable high-throughput spatial analysis on GeoMx® Digital Spatial Profiler (DSP) using the Whole Transcriptome Atlas (WTA) and immuno-fluorescent morphology markers: SYTO82 (nuclei), CAIX (hypoxia), pan-cytokeratin (epithelium), CD3 (T-cells). A.I.-based analysis (Oncotopix® Discovery) of serial section H&E images and GeoMx IF images was developed to identify ROIs for GeoMx collection. Immune hot and cold selection used leukocyte density, tumor/stroma interface selection used epithelial areas. Areas of illumination (AOI) were chosen using concentric CAIX expression gradients. Integrated analysis of digital images using Oncotopix Discovery and the whole transcriptome was done to assess the above TME compartments.

Results: Automated ROI placement based on tumor/stroma, hypoxia and immune infiltration and AI /Deep Learning based AOI segmentation reduced AOI selection time and improved accuracy of tissue compartment enrichment, especially between samples and tissue types. Automated development of hypoxia gradient-based AOI enabled a selection strategy not possible in the standard DSP software. Cell phenotyping using IF morphology scan was used to supervise cell deconvolution.

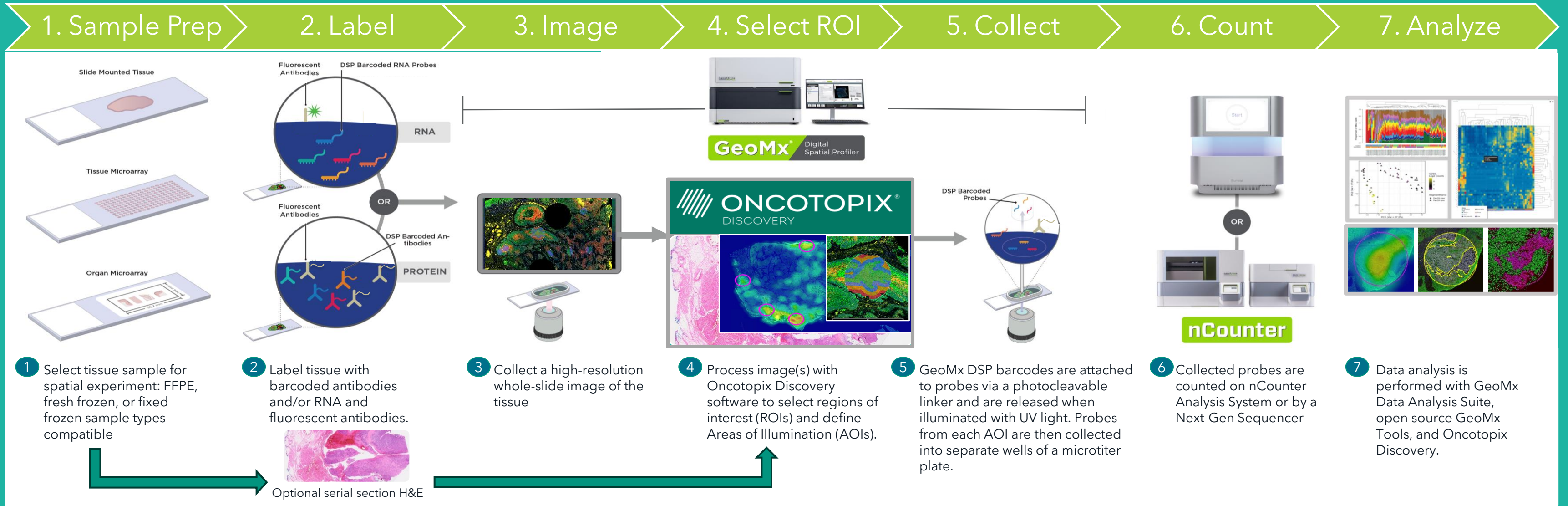
Conclusions: This work shows that ROI-based spatial analyses can be used to explore the effects of hypoxia levels on immune infiltration in HNC. Automated AI-based ROI selection provides a means of sampling relevant tumor subtypes based on hypoxia and immune infiltrate criteria in an unbiased, reproducible manner, and can provide a standardized, automated method for selecting ROIs and segmenting AOIs across a cohort of mixed tissue types and pathological subtype, improving throughput.

Methods



Slide label	Molecular Subgroup	Hypoxia-immune subgroup	CD3+ (scored 1-12 low to high)	CA-IX+ (% of tumour cells positive)	PD-L1+ tumour (% cells positive)	PD-L1+ immune cells	PD-L1+ cordon
1A	2	Hypoxia ^{high} /Immune ^{low}	5.33	70	20	low	Yes
1B	3	Mixed	9.67	15	55	low	No
2A	2	Hypoxia ^{high} /Immune ^{low}	5.33	67.5	0	low	No
2B	1	Hypoxia ^{low} /Immune ^{high}	11.33	20	25	low	No
3	1	Hypoxia ^{low} /Immune ^{high}	12.00	2.5	17.5	low	No
4	3	Mixed	6.33	35	25	high	Yes

AI-driven Digital Spatial Profiling



ROI & AOI Selection

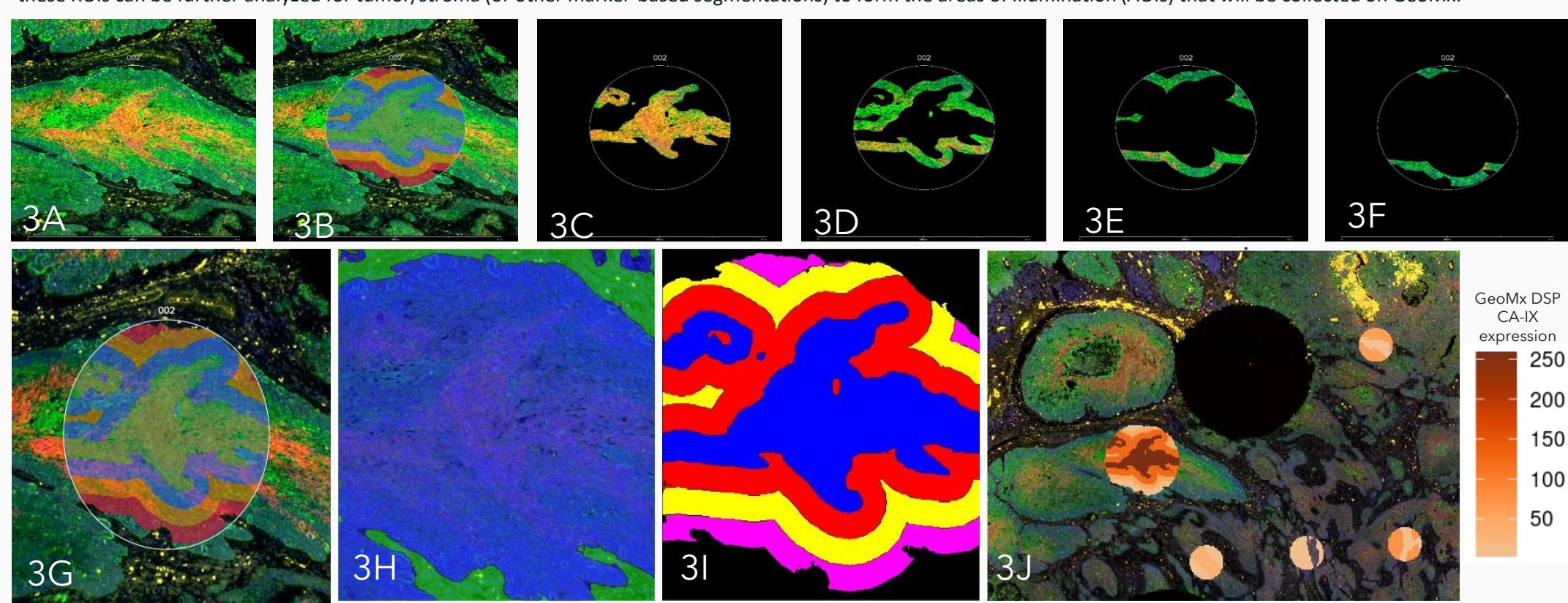
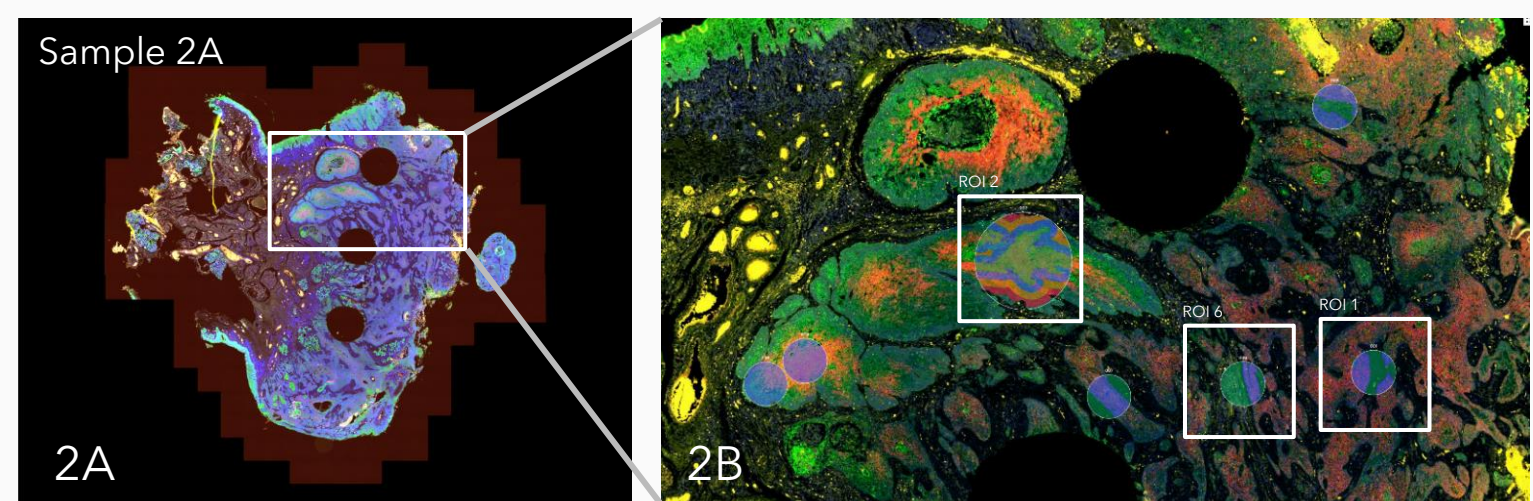
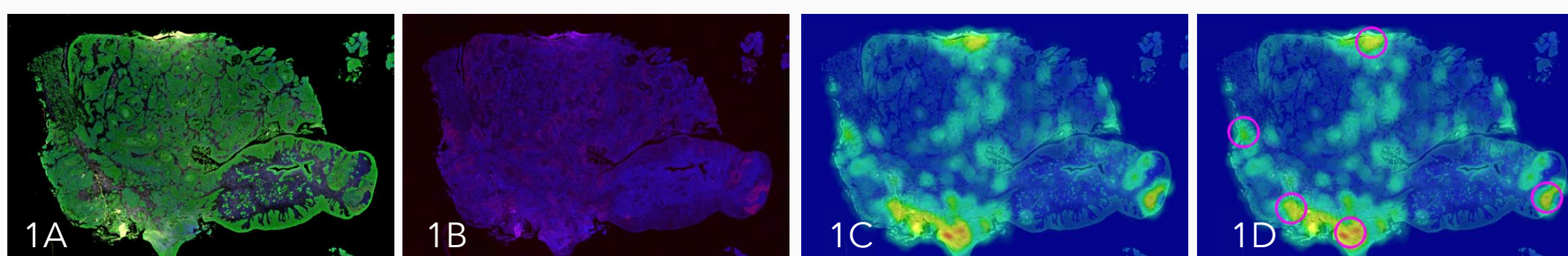


Figure 2: Creating AOIs from CA-IX hotspots using two different methods. 2A shows a whole-slide 4-color IF images taken on a GeoMx of Sample 2A. 2B shows a zoomed-in portion of the whole slide. For this sample, 7 circular hotspots were chosen to be ROIs. These can be seen superimposed on the color IF image. ROIs 1 and 3-7 were segmented using a paint-to-train deep-learning-based approach into tumor and stromal regions (see Figure 4). ROI 2 was created larger than the others, was segmented into tumor and stroma, and then the tumor region segmented into a very high CA-IX-expression region and the rest. The high CA-IX region was expanded in 50 um steps to form concentric regions around the CA-IX hotspot. An expanded view of this process can be seen in Figure 3.

Figure 3: Generating AOIs using staining intensity gradients. This is the first of two methods used to generate AOI. 3A shows the 4-color IF image of ROI 2 in Sample 2A. 3B and 3G show the result of taking a CA-IX hotspot region (in green at the center of the circle) and expanding that region in 50 um increments to form a concentric gradient around the CA-IX hotspot. The concentric regions are shown in as overlays in 3B and 3G as green > blue > orange > red in terms of CA-IX intensity. In addition, this ROI was also analyzed for tumor/stroma, which is shown in 3H, with blue being tumor areas and green being stromal areas. The concentric CA-IX gradients are shown in 3I only for the tumor region (blue, red, yellow, magenta). Each of these gradient regions was then used to form a separate AOI for data collection on GeoMx. These 4 individual AOIs can be seen in 3C, 3D, 3E, and 3F. CA-IX expression by GeoMx confirms IF expression gradients (3J).

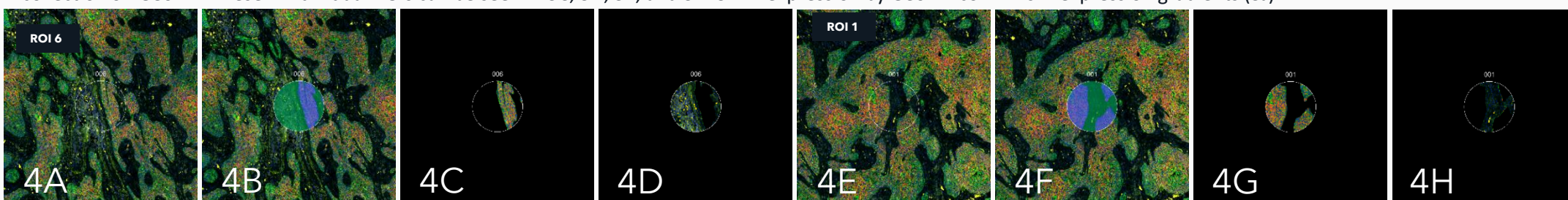


Figure 4: Creation of AOIs based on tumor/stroma tissue segmentation. This is the second method for the generation of AOIs. In this case, each circular ROI was segmented using a paint-to-train deep-learning-based approach into tumor and stromal regions, each of which became an AOI for GeoMx data collection. 4A through 4D show the sequence for ROI 6 of Sample 2A. The circular ROI was segmented into tumor (blue) and stroma (green), and each AOI is shown in 4C (tumor) and 4D (stroma). Figures 4E through 4H show the same sequence of steps for ROI 1 of Sample 2A.

Deep Learning Segmentation

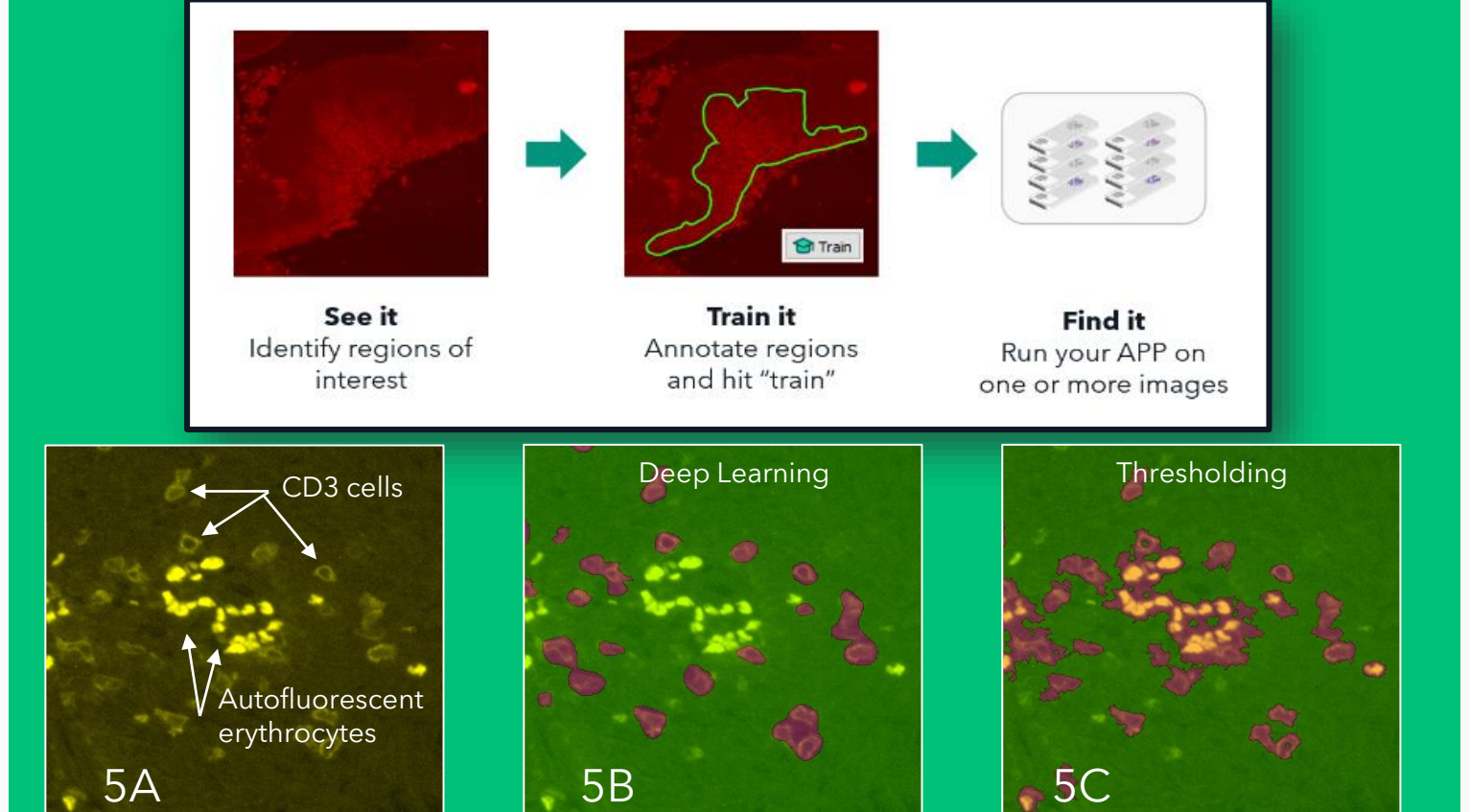


Figure 5: Comparison of Deep Learning techniques (Visiopharm) versus threshold techniques (GeoMx standard workflow) for CD3+ cell detection. Visiopharm's deep-learning-based approaches are quite flexible and can be used to address many different cell and tissue segmentation problems such as separating CD3 positive cells from autofluorescent erythrocytes (5A). In this case, a Deep Learning APP was trained to detect CD3+ cells and exclude autofluorescence including erythrocytes (5B). Note that bright objects are automatically excluded. Post processing steps provide the flexibility to exclude based on shape or size, and also to add a "watershed" region around small objects to prevent overlap of signal. By comparison, an intensity threshold approach (cutoff 95) was used to create a threshold mask (5C). Note that both erythrocytes and CD3+ cells are included when only using thresholding.

Whole Transcriptome Analysis

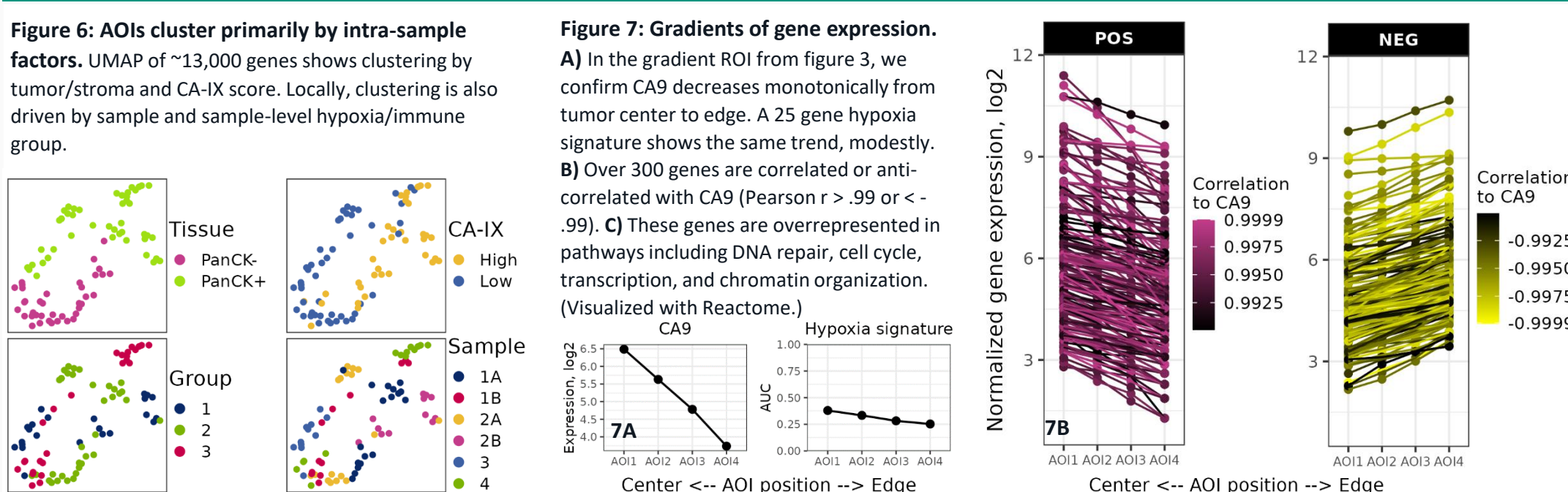


Figure 6: Genes differentially expressed between tumor and TME. A) Select genes implicated in HNC, other cancers, hypoxia, and tumor microenvironment are shown in boxplots. Fold change is >2 or <-2 and FDR < .05 for all genes shown. B) Differential expression was determined with a LMM using sample-level immune/hypoxia groups and sample as random effects. CA-IX high/low intra-tissue regions were not considered. Sample size is small and warrants further investigation.

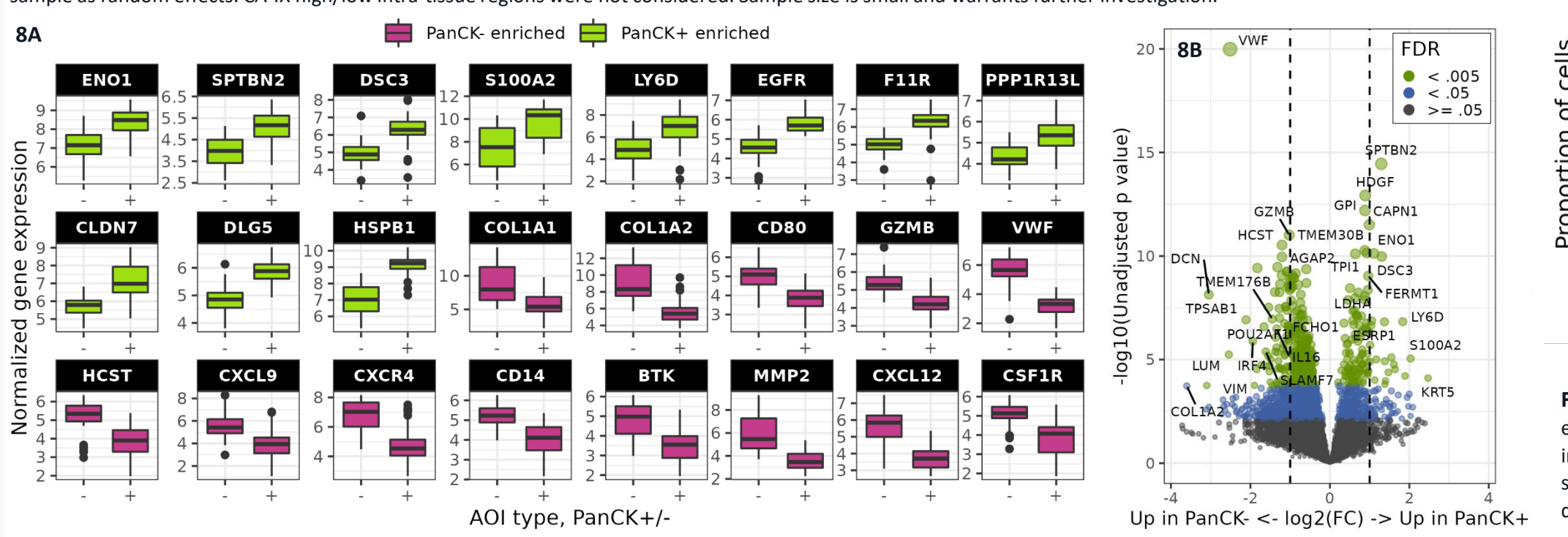


Figure 7: Gradients of gene expression. A) In the gradient ROI from figure 3, we confirm CA9 decreases monotonically from tumor center to edge. A 25 gene hypoxia signature shows the same trend, modestly. B) Over 300 genes are correlated or anti-correlated with CA9 (Pearson r > .99 or < -.99). C) These genes are overrepresented in pathways including DNA repair, cell cycle, transcription, and chromatin organization. (Visualized with Reactome.)

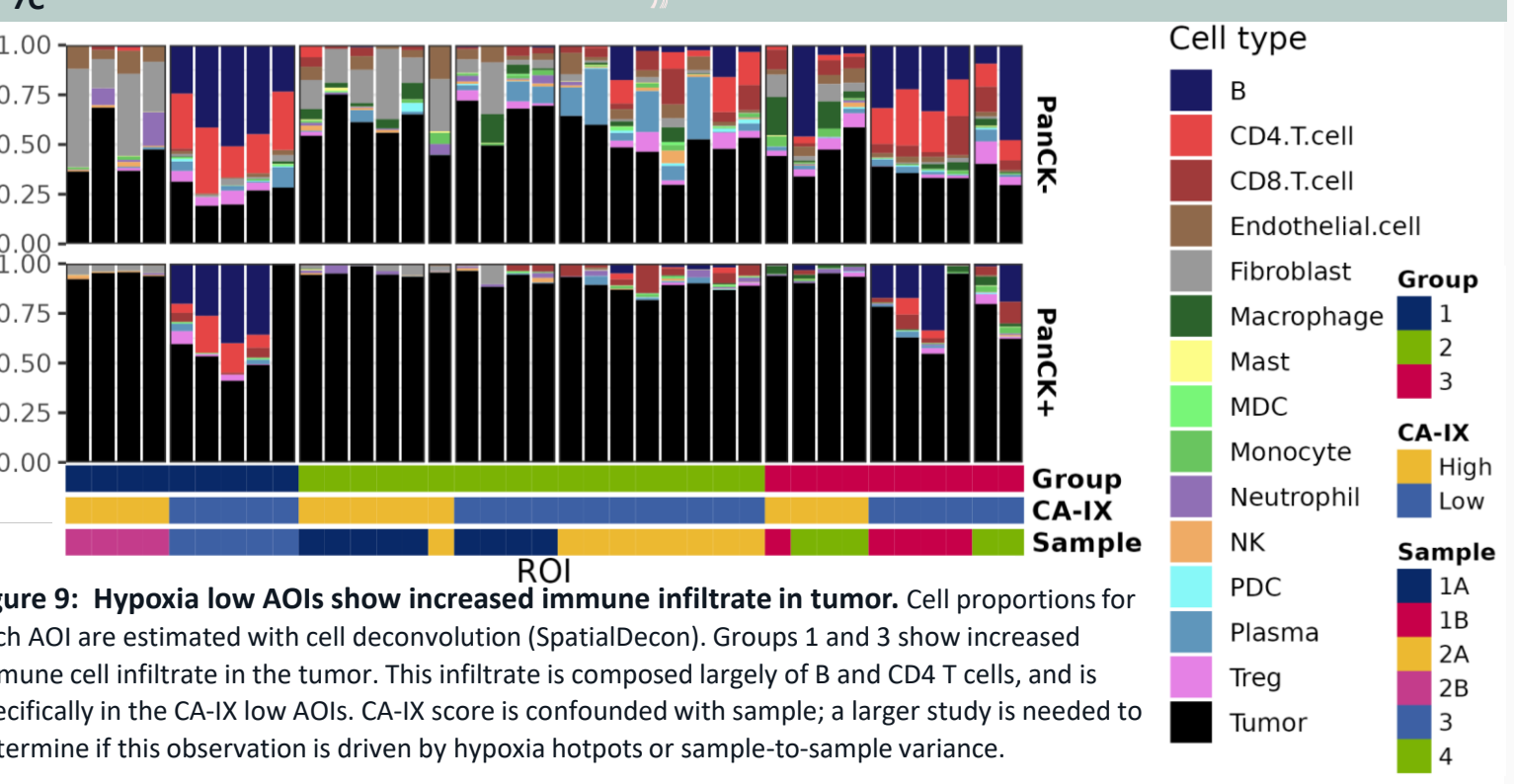
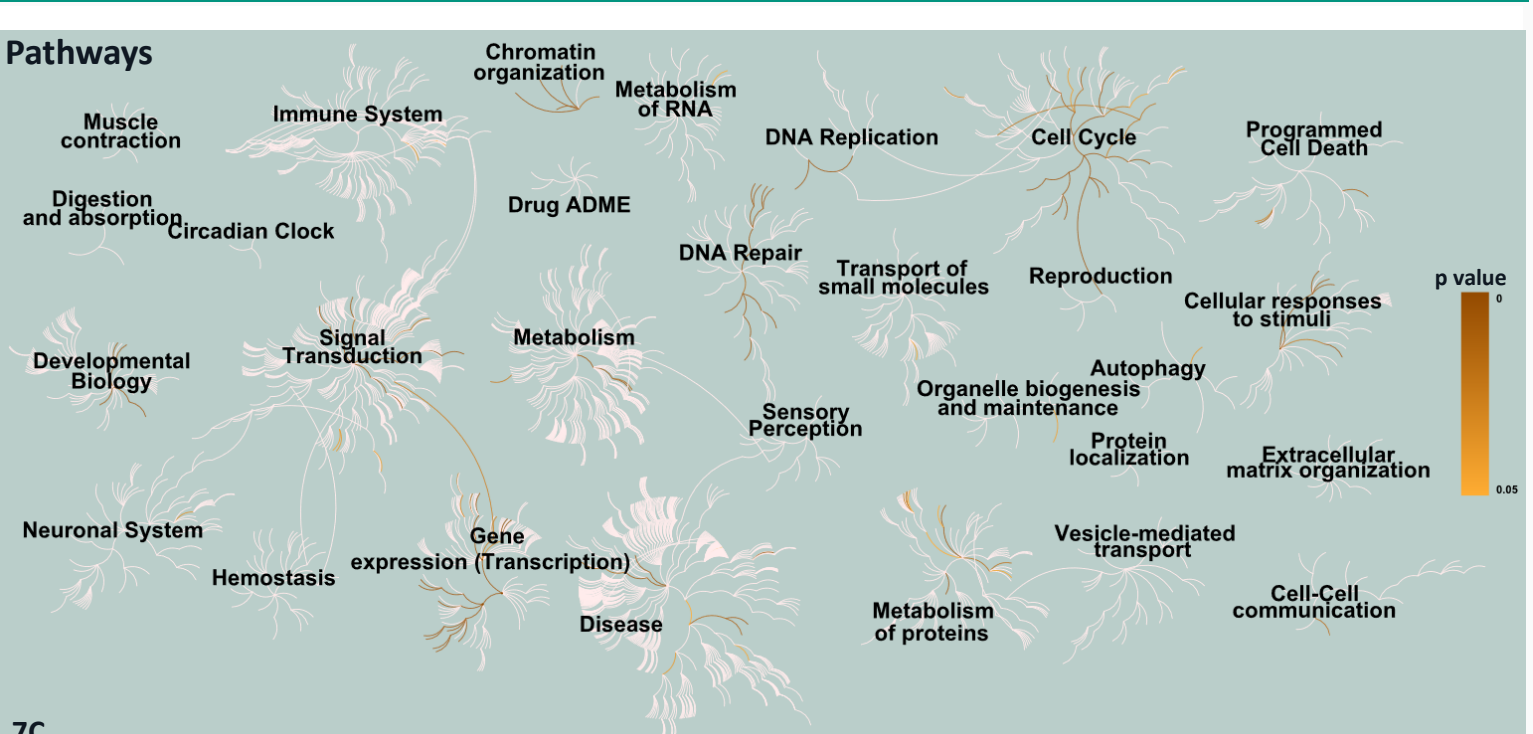


Figure 9: Hypoxia low AOIs show increased immune infiltrate in tumor. Cell proportions for each AOI are estimated with cell deconvolution (SpatialDecon). Groups 1 and 3 show increased immune cell infiltrate in the tumor. This infiltrate is composed largely of B and CD4 T cells, and is specifically in the CA-IX low AOIs. CA-IX score is confounded with sample; a larger study is needed to determine if this observation is driven by hypoxia hotspots or sample-to-sample variance.

Post-GeoMx IF Image Analysis

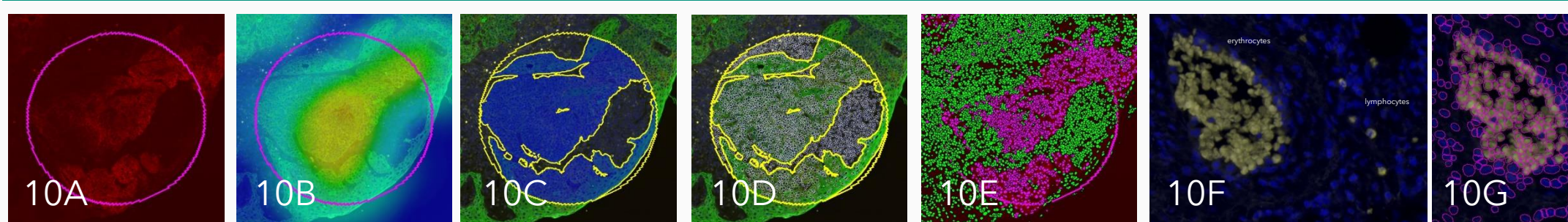


Figure 10: Cellular analysis of ROIs and AOIs. ROIs and the AOIs inside them were analyzed using a deep-learning-based cellular segmentation using the syto82 as the nuclear marker and a paint-to-train tissue segmentation. First, CA-IX staining (10A) was visualized as a heatmap (10B). The ROI showing the tumor mask and tumor cells in green (10C). Cells within the entire ROI were segmented using a pre-trained APP for nuclear detection (10D). Cells were classified into tumor or stromal cells using a deep learning network (10E). The power of this deep learning network is seen in 10F and 10G. 10F shows the CD3 channel in yellow, but both erythrocytes and CD3+ cells can be seen. 10G shows the result of the cellular classification, showing only cells positive for CD3 marked as CD3+ (green outlines).

Image	Stroma Counts (CD3+)	Stroma Counts (CD3-)	Tumour Counts (CD3+)	Tumour Counts (CD3-)	ROI	Stroma Area [um ²]	Tumour Area [um ²]
Tissue 2A	2	190	2	390	ROI 001	31126	39568
Tissue 2A	0	95	0	481	ROI 003	6284	64381
Tissue 2A	0	37	2	1115	ROI 004	2351	68345
Tissue 2A	0	18	6	1190	ROI 005	1137	69542
Tissue 2A	2	603	1	248	ROI 006	47741	22966
Tissue 2A	0	221	0	425	ROI 007	31044	39652
Tissue 2A	1	247	2	503	ROI 008	21532	49147
Tissue 2A	4	203	0	368	ROI 009	30554	40109
Tissue 2A	1412	148691	390	171425	Whole of 2A	18097862	16137832

Summary

- The GeoMx DSP system is an excellent spatial biology acquisition system, but manual selection of ROIs can be time-consuming.
- We have created a method to automatically place ROIs and AOIs for GeoMx Digital Spatial Profiling using Visiopharm's Oncotopix Discovery software which will enable large scale studies by increasing throughput.
- Use of AI to assist in ROI and AOI selection reduces selection bias and time and can increase cellular enrichment for profiling.
- Immune infiltrate in the hypoxia-low tumour AOIs consists largely of B and CD4 T cells.
- An expanded cohort analysis is planned.